Semibatch Emulsion Copolymerization of Methyl Methacrylate and Butyl Acrylate

C. S. CHERN* and H. HSU

Department of Chemical Engineering, National Taiwan Institute of Technology, Taipei, Taiwan, Republic of China

SYNOPSIS

The concentration of sodium lauryl sulfate (SLS) in the initial reactor charge is the most important parameter in determining the particle size of a semibatch emulsion copolymerization of methyl methacrylate (MMA) and butyl acrylate (BA). The number of particles formed is proportional to the concentration of SLS to the 0.5–1.2 power and it is proportional to the concentration of the nonyl phenol–40 mol ethylene oxide adduct to the 0.014–0.72 power. The number of particles is almost independent of the concentration of the initiator. The solubility of monomer in water has an important effect on the nucleation mechanism according to the literature. However, the ratio of MMA to BA does not show any significant effect on the latex particle size in our laboratory. The particle size also increases with increasing ionic strength or agitation speed. Experimental data of particle-size distribution and molecular weight distribution support the coagulative nucleation mechanism when the concentration of SLS is way below its critical micelle concentration (CMC). © 1995 John Wiley & Sons, Inc.

INTRODUCTION

Emulsion polymerization is a heterogeneous system in which most of the chain propagation reaction occurs in segregated particles (50–1000 nm in diameter) dispersed in water. These numerous particles collide with each other frequently and tend to aggregate due to the attractive van der Waals forces. Stability against aggregation can be achieved by the addition of an anionic surfactant that imparts repulsive forces between similarly charged electric double layers to the emulsion polymer. Latex products are widely used in coatings, adhesives, thermoplastics, and rubber industries.

Control of the latex particle size is the key to guarantee the quality of latex products. For example, the rheological property is dependent on the particle-size distribution. Changes in the viscosity due to batch-to-batch variations might cause production problems to the tape and label manufacturers. In addition, the primary functions of trade paints and industrial coatings are protection and decoration. The particle-size distribution plays an important role in the application properties of these latex products. Although the particle nucleation period is quite short in the course of emulsion polymerization, this period ultimately determines the final particle size. In the past 40 years, several nucleation mechanisms were proposed: micellar nucleation,[1–3] homogeneous nucleation,[4–6] coagulative nucleation,[7,8] and emulsified monomer droplet nucleation.[9,10]

Semibatch emulsion polymerization is one of the most important processes for the production of polymeric materials because of limitations of heat transfer in the large-scale reactor. Most of the literature dealing with the particle nucleation and growth processes is confined to batch emulsion polymerization. Novak[11] studied the semibatch emulsion copolymerization of methyl methacrylate (MMA) and butyl acrylate (BA). The reaction system was stabilized by an anionic surfactant, sodium dodecylbenzene sulfonate. Based on the coagulative nucleation mechanism, he developed a simple model to describe the particle nucleation and growth. The model predicts that the final particle size is proportional to the concentration of the surfactant to the $-\frac{1}{3}$ power. It is interesting to extend the model to the formulation using mixed surfactants (i.e., an an-

* To whom correspondence should be addressed.

Journal of Applied Polymer Science, Vol. 55, 571–581 (1995)
 CCC 0021-8995/95/040571-11

ionic surfactant in combination with a nonionic surfactant).

The objective of this work was to investigate the effect of various reaction parameters on the particle nucleation and growth for the emulsion copolymerization of MMA/BA in a semibatch reactor. The reaction parameters include the ratio of MMA to BA, concentration of sodium lauryl sulfate (SLS) in the initial reactor charge, concentration of the nonyl phenol–40 mol ethylene oxide adduct (NP-40) in the initial reactor charge, concentration of the initiator in the initial reactor charge, concentration of SLS in the monomer emulsion feed, ionic strength, and agitation speed.

EXPERIMENTAL

The chemicals used were methyl methacrylate (MMA) (Kaohsiung Monomer Co.), butyl acrylate (BA) (Formosa Plastics Co.), sodium lauryl sulfate (SLS) (Henkel Co.), nonyl phenol–40 mol ethylene oxide adduct (NP-40) (Union Carbide), sodium persulfate (Riedel-de-Haen), sodium chloride (Riedel-de-Haen), nitrogen (Ching-Feng-Harng Co.), and deionized water.

Polymerization was carried out in a 1 L glass reactor equipped with an agitator, a thermometer, and a condenser. All process water along with the initial surfactant and monomer were charged to the reactor at room temperature. The initial reactor charge was purged with nitrogen for 10 min while the reactor temperature was brought to 80°C. The reaction was then initiated by adding the initiator solution to the reactor. After 15 min, the monomer emulsion was fed to the reactor over 180 min by an FMI pump. Polymerization temperature was kept constant (80°C) throughout the reaction. After the monomer emulsion feed was complete, the reaction system was kept at 80°C for 30 min to reduce the residual monomer. The theoretical total solids content at the end of the reaction is 40%.

The finished batch was filtered through a 40 mesh (0.42 mm) and a 200 mesh (0.074 mm) screen in series to collect the filterable solids. Scraps that adhered to the agitator, thermometer, and reactor wall were also collected. Total solids content was determined by the gravimetric method. Particle-size distribution data were obtained from the dynamic light-scattering method (Otsuka Photal LPA-3000/3100) and transmission electron microscope (TEM, Hitashi H-7100). Molecular weight distribution was determined by gel permeation chromatography (GPC, Gilson Model 116 & 132 detector, Ultrastyragel 7.8 × 300 mm Waters columns).

RESULTS AND DISCUSSION

The Plackett–Burman experimental design[12] (six variables/12 experiments) was used to screen the polymerization variables selected for study. These variables include (1) concentration of SLS in the initial reactor charge (0.01–0.5% on water), (2) concentration of SLS in the monomer emulsion feed (2.3–4.0% on total monomer), (3) concentration of NP-40 in the initial reactor charge (0.01–0.5% on water), (4) concentration of initiator in the initial reactor charge (0.1–0.4% on water), (5) MMA/BA ratio (30/70–70/30), and (6) concentration of monomer in the initial reactor charge (3–6% on water).

To test the batch-to-batch variations, one experiment taken from the Plackett–Burman design (recipe: 0.5% SLS in the initial reactor charge, 4.0% SLS in the monomer emulsion feed, 0.5% NP-40 in the initial reactor charge, 0.4% $Na_2S_2O_8$, 70% MMA, and 6% initial monomer charge) was carried out twice. The average particle size of the finished batches was 80 ± 2 nm. Another experiment selected from the two-level factorial design shown below (recipe: 0.01% SLS in the initial reactor charge, 0.01% NP-40 in the initial reactor charge, and 0.08% $Na_2S_2O_8$) was carried out four times. The average particle size of the finished batches was 343 ± 25 nm. The reproducibility of both formulas, which result in very different particle sizes, is good.

The overall average particle size of the finished batches of the Plackett–Burman design is 145.6 nm. The effect of each variable on the particle size is (1) −141.1, (2) −26.9, (3) −61.6, (4) 10.7, (5) −6.7, and (6) 1.1. The numerical value corresponding to the variable represents the effect of the variable on the particle size when the variable is changed from the minus level to the plus level and the units are in nanometers. The greater the number, the stronger the effect of the variable on the particle size. The standard error of a factor effect is 25.8 nm. Experimental data show that variables (1) and (3) influence the particle size the most. The anionic surfactant SLS in the initial reactor charge is the major particle generator. NP-40 acts as an auxiliary stabilizer. The higher the concentration of SLS and NP-40 in the initial reactor charge, the smaller the particle size. The concentration of SLS in the monomer emulsion feed does not affect the particle

size very much and its primary function is to stabilize the growing particles. Addition of SLS to the reactor during the monomer emulsion feed might cause secondary nucleation, as shown by its effect: −26.9 nm.

The micellar, homogeneous, and coagulative nucleation mechanisms all predict that the number of particles formed during nucleation is proportional to the concentration of the initiator to the $\frac{2}{5}$ power (i.e., the particle size is proportional to the concentration of the initiator to the −0.13 power). However, the Plackett–Burman design shows that the effect of initiator concentration in the initial reactor charge on the particle size is insignificant. The role of initiator in the semibatch emulsion polymerization will be reexamined later.

The solubility of MMA in water is about 15 times greater than that of BA.[13] Experimental data show that the MMA/BA ratio does not have a significant effect on the particle size. In addition, the concentration of monomer in the initial reactor charge also shows very little effect on the particle size. These observations can be explained by the fact that SLS and NP-40 in the initial reactor charge predominate in the nucleation of primary particles. The filterable solids and reactor scraps for the designed experiments are relatively low because the level of SLS in the monomer emulsion feed is sufficient to protect the growing particles against flocculation.

We then chose variables (1), (3), and (4) as the variables of a two-level factorial design (nine experiments, one midpoint included) to quantitatively analyze the effects of these variables on the particle size. Again, the data show that the level of SLS in the initial reactor charge is the most important parameter and the initiator almost has no influence on the particle size. The nonionic surfactant NP-40 acts as an auxiliary surfactant and it is especially effective for promoting the chemical and freeze-thaw stability. Based on the factorial design, we derived a prediction equation for the particle size. Figure 1 shows the contour plot of particle size constructed from the prediction equation (initiator concentration = 0.08%). The contour plots at various initiator levels show a similar trend. The abscissa is the concentration of NP-40 in the initial reactor charge and the ordinate is the concentration of SLS in the initial reactor charge. In considering the curves with size less than 90 nm, the level of SLS required to maintain the same size remains relatively constant when the concentration of NP-40 is less than 0.2%. This is because SLS predominates in the particle nucleation process. On the other hand, the level of SLS required to maintain the same size drops when the concentration of NP-40 is greater than 0.4% since NP-40 becomes important in this region.

Considering the curves with size less than 70 nm, the level of NP-40 should increase with increasing SLS in order to maintain the same particle size. This is probably due to the increasing ionic strength associated with an increase in the SLS loading. The increasing electrolyte concentration can cause a decrease in the potential energy barrier against flocculation between two particles. The resultant-lim-

Table I Experiments Designed to Verify the Prediction Equation of Particle Size (Initiator Concentration = 0.08%)

	L	M	S
SLS (%)	0.02	0.19	0.49
NP-40 (%)	0.02	0.15	0.39
Prediction (nm)	330	210	80
Experimental data (nm)[a]	282.1	107.2	77.4
Error (%)	−14.5	−49.0	−3.3
15 Min sample			
u/G^2 [b]	−0.0092	0.058	0.092
d_w/d_n [c]	1.01	1.24	1.54
Final sample			
u/G^2 [b]	−0.04	0.0075	0.037
d_w/d_n [c]	1.01	1.01	1.01

[a] Dynamic light scattering method.
[b] Monodisperse when $u/G^2 < 0.1$.
[c] Polydispersity index.

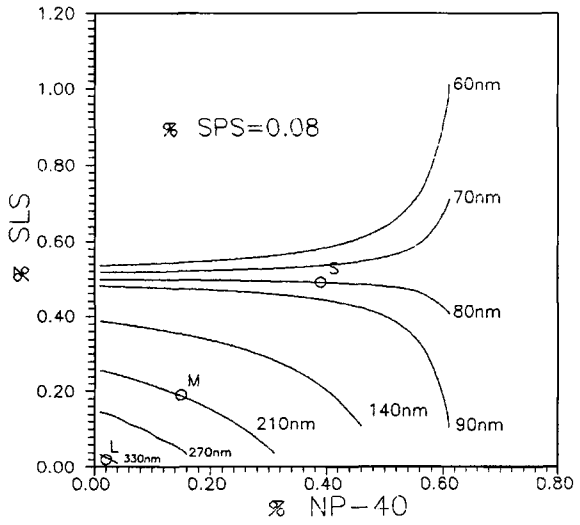

Figure 1 Contour plot of latex particle size: initiator concentration = 0.08%.

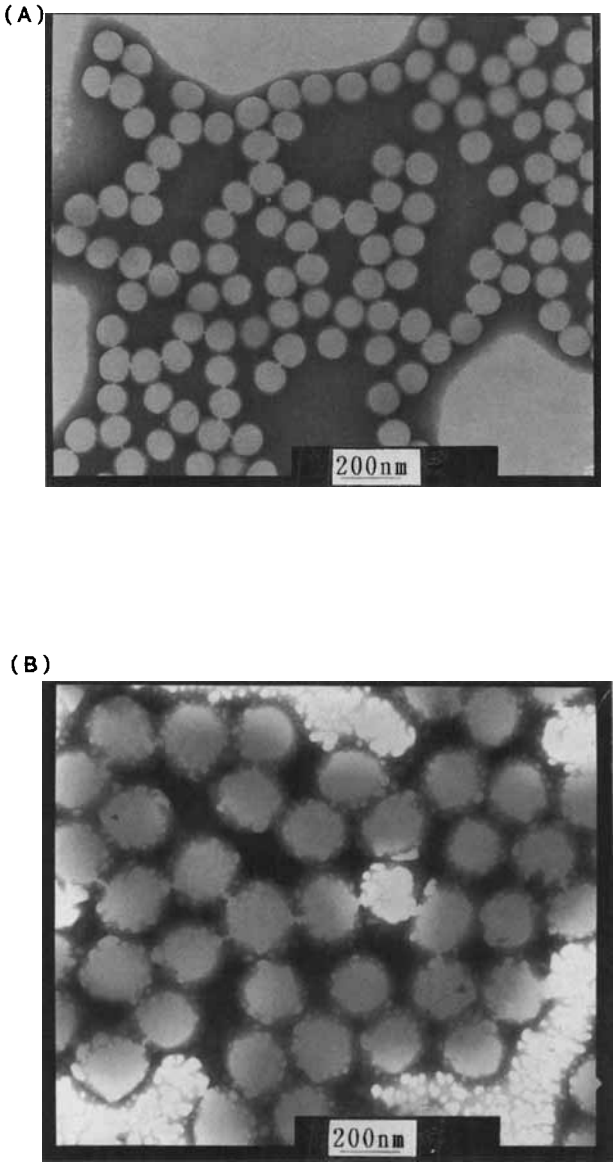

Figure 2 TEM photographs of experiment L: (A) 15 min sample; (B) final latex sample.

ited flocculation process may lead to a larger particle size than expected. Please note that this behavior occurs just outside the designed box and its validity requires experimental justification.

We selected three points (L, M, and S) in Figure 1 to verify the particle-size prediction equation. The formulas and experimental results are listed in Table I. The experimental data agree reasonably well with the prediction except for experiment M. This is probably because there is only one midpoint in the factorial design and the design fails to predict the curvature accurately. Figures 2–4 show the TEM photographs of the three runs L, M, and S, respectively. Figure 4(A) shows serious agglomeration during TEM sample preparation. Experiment L has the lowest surfactant concentration in the initial reactor charge and, consequently, it should have the shortest nucleation time. On the other hand, experiment S has the highest surfactant concentration and, hence, the longest nucleation time. Thus, the polydispersity indices of the 15 min particle-size distribution data in the decreasing order are S > M > L, as shown by Table I and Figures 2–4. The final particle-size distributions of latexes L, M, and S all have the same polydispersity index because the residence time distribution for the growing particles in

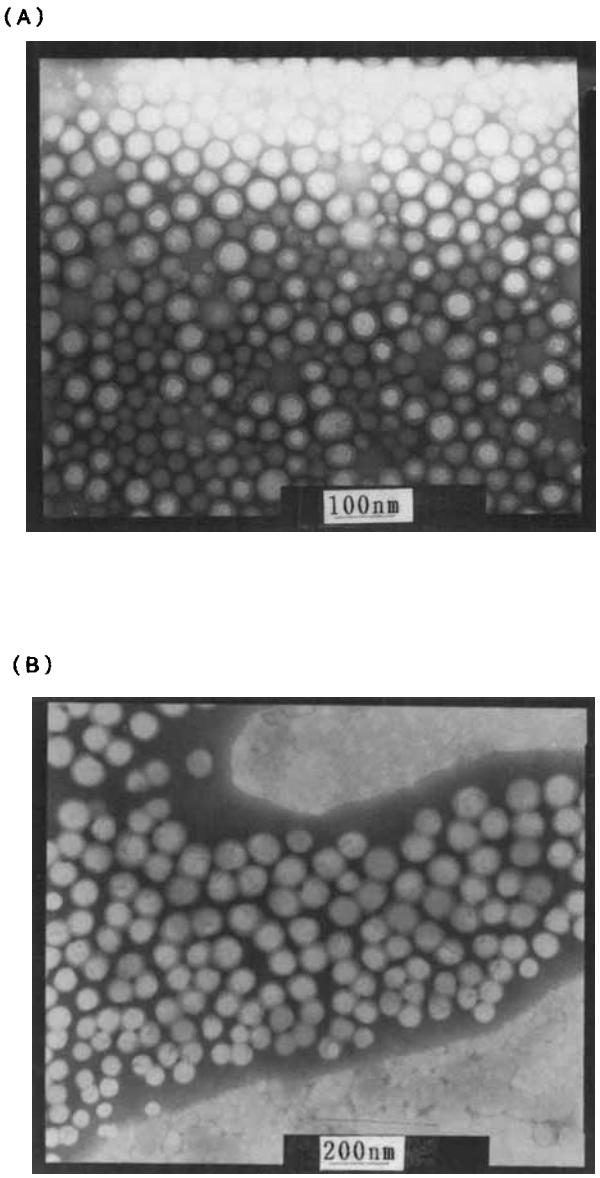

Figure 3 TEM photographs of experiment M: (A) 15 min sample; (B) final latex sample.

(A)

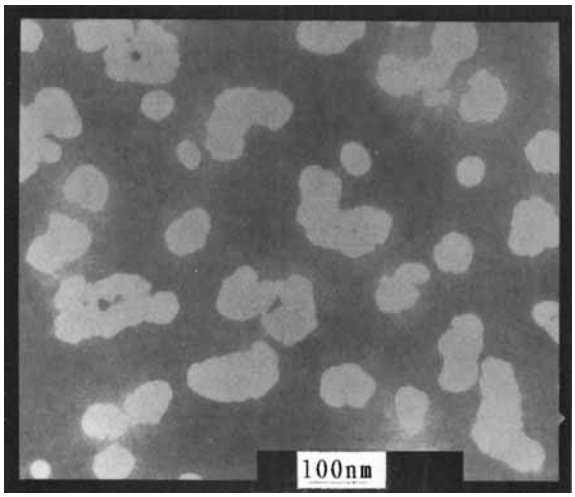

(B)

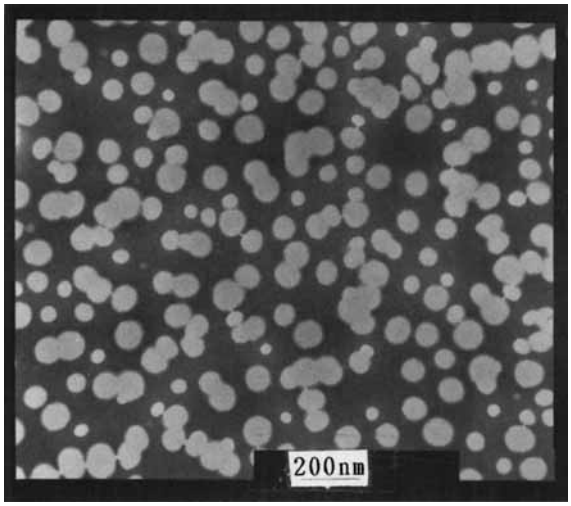

Figure 4 TEM photographs of experiment S: (A) 15 min sample; (B) final latex sample.

the reactor becomes narrower as polymerization proceeds. For the finished batch of latex L, there are a number of tiny particles surrounding the large particles as shown in Figure 2(B), since the surface area of latex L is not large enough to prevent the secondary nucleation from occurring during the monomer emulsion feed. This observation is similar to Vanderhoff et al.'s experimental results.[14]

Feeney et al.,[15] based on the coagulative nucleation mechanism, showed that immediately after the nucleation was complete the fraction of particles having volume v plotted against v was positive-skew. Figure 5(A) shows that experiment L using the lowest concentration of surfactants displays such a positive-skew distribution. The data for latexes M and S shown in Figure 5(B) and (C) cannot be used to support the coagulative nucleation mechanism because of the observed bimodal particle-size distribution. Figure 6 shows the log N_f-vs.-log SLS curves at three initiator concentrations (0.08, 0.265, and 0.45%), where N_f is the number of particles per liter water and SLS is the concentration of SLS in the initial reactor charge. The effect of SLS on N_f depends on the concentration of NP-40 and the slope of the log N_f-vs.-log SLS plot ranges from 0.5 to 1.2. According to the micellar or homogeneous nucleation mechanism, the slope of the log N_f-vs.-log SLS plot equals 0.6, whereas Feeney et al.[15] showed that the slope of the log N_f-vs.-log SLS plot should lie between 0.4 and 1.2.

Figure 7 shows the log N_f-vs.-log NP-40 plot at three initiator concentrations (0.08, 0.265, and 0.45%), where NP-40 is the concentration of NP-40 present in the initial reactor charge. Similarly, the effect of NP-40 on N_f depends on the concentration of SLS and the slope of the log N_f-vs.-log NP-40 plot ranges from 0.014 to 0.72. Figure 8 shows the log N_f-vs.-log SPS plot at three NP-40 concentrations (0.01, 0.255, and 0.5%), where SPS is the concentration of the initiator in the initial reactor charge. N_f increases with increasing SPS when the concentration of SLS is high, but the effect is not significant, whereas N_f decreases with increasing SPS when the concentration of SLS is low, which is consistent with the results of Sutterlin et al.[13] During nucleation, the stability of the primary particles is limited since the amount of surfactants available for stabilization is quite low. An increase in the ionic strength associated with increasing SPS can lead to limited flocculation and reduce the number of particles nucleated.

Chu and co-workers[16,17] studied the effect of mixed surfactants (anionic and nonionic surfactants) on the latex particle size and derived the following equation:

$$TS_m = c + d(TS_a + TS_i)$$
$$= c + \alpha_a E_a^{b_a} + \alpha_n E_n^{b_n} \quad (1)$$

where TS is the total particle surface area, E is the amount of surfactant used, and c, d, α_a, α_n, b_a, and b_n are constants. The subscripts m, a, and n represent the mixed, anionic, and nonionic surfactants, respectively. Based on our experimental data, we employed the nonlinear least-squares best-fit

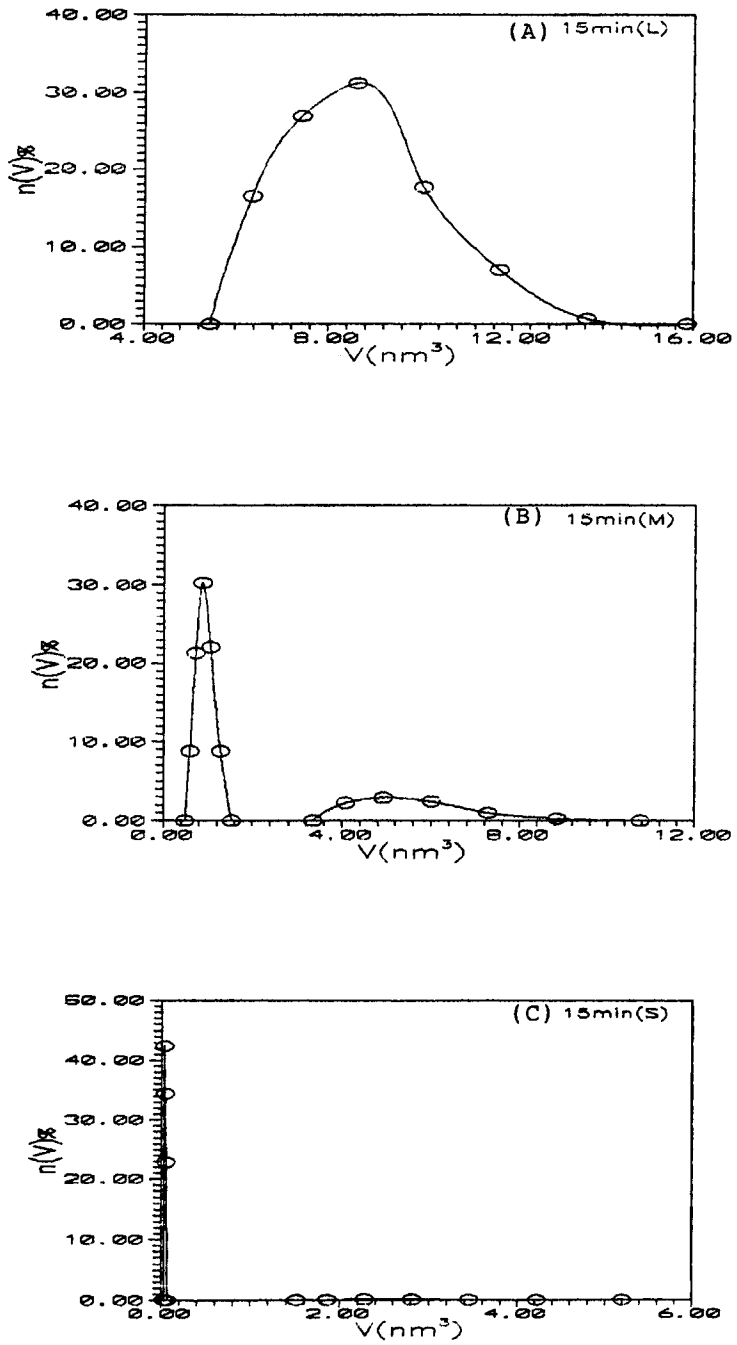

Figure 5 Particle-size distribution data of 15 min samples determined by dynamic light scattering method: (A) experiment L; (B) experiment M; (C) experiment S.

method to obtain c, α_a, α_n, b_a, and b_n for the MMA/BA (50/50) system. The calculated parameters along with Chu and co-worker's data are compiled in Table II. α_a is approximately one order of magnitude greater than α_n, which means that the anionic surfactant is more important than is the nonionic surfactant in the particle nucleation process.

Based on the coagulative nucleation mechanism, Novak[11] assumed that the particle surface was saturated with surfactant and there was no flocculation and secondary nucleation taking place during the monomer feed and he developed a simple model to describe the particle nucleation and growth processes. His model predicts that the slope of the log

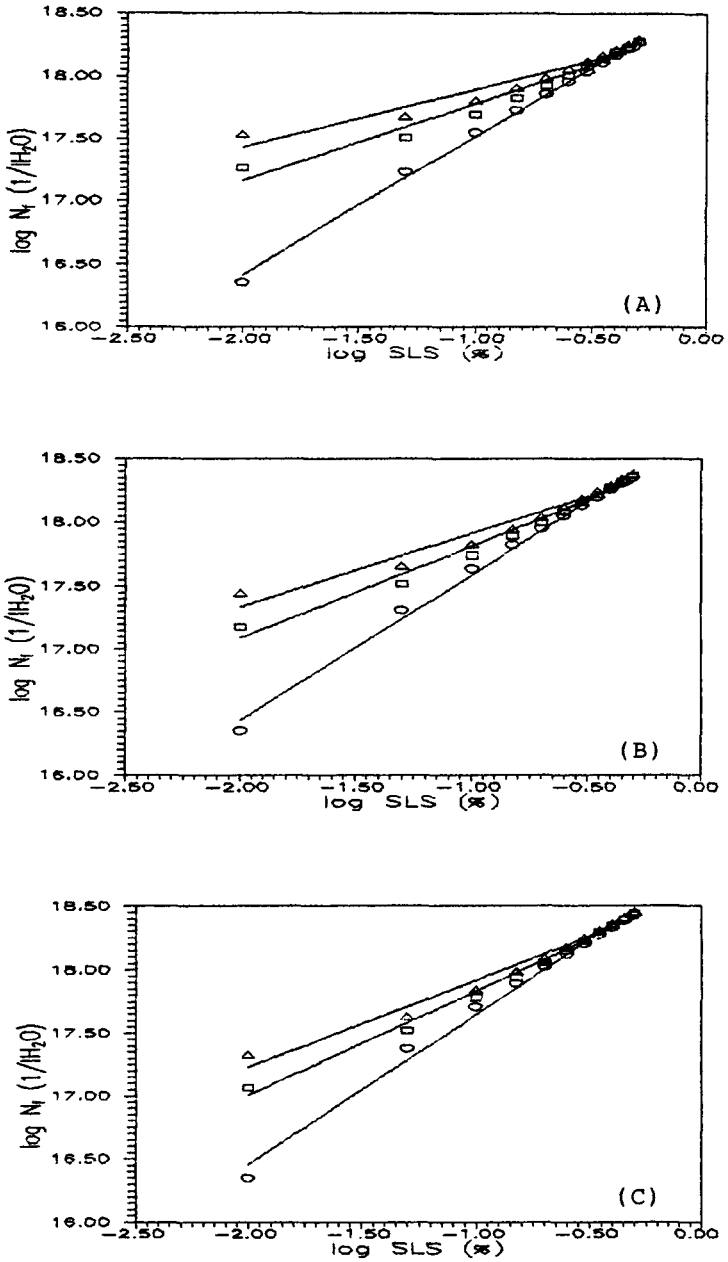

Figure 6 No. particles vs. concentration of SLS curves: (△) NP-40 = 0.5%; (□) NP-40 = 0.255%; (○) NP-40 = 0.01%. (A) Initiator concentration = 0.08%; (△) slope = 0.464; (□) slope = 0.621; (○) slope = 1.106. (B) Initiator concentration = 0.265%; (△) slope = 0.574; (□) slope = 0.724; (○) slope = 1.154. (C) Initiator concentration = 0.45%; (△) slope = 0.688; (□) slope = 0.826; (○) slope = 1.193.

D_f-vs.-log$(1/G_a)$ plot should be $\frac{1}{3}$, where D_f was the final particle size, and G_a, the amount of anionic surfactant used during nucleation. We extended the Novak model to the case of mixed surfactants and derived the following equation:

$$\log D_f = \tfrac{1}{3} \log[1/(G_a A_a + G_n A_n)] + \tfrac{1}{3} \log N' \quad (2)$$

where $N' = 6D_{pp}^2 G_f/\rho$. D_{pp} is the primary particle diameter; G_f, the final particle weight; ρ, the polymer density; G_n, the amount of nonionic surfactant used; and A_a and A_n, the particle surface area covered by 1 g of anionic and nonionic surfactant, respectively.

A_a and A_n are estimated to be 1.412×10^{21} and 0.480×10^{21} nm^2/g, respectively, according to the

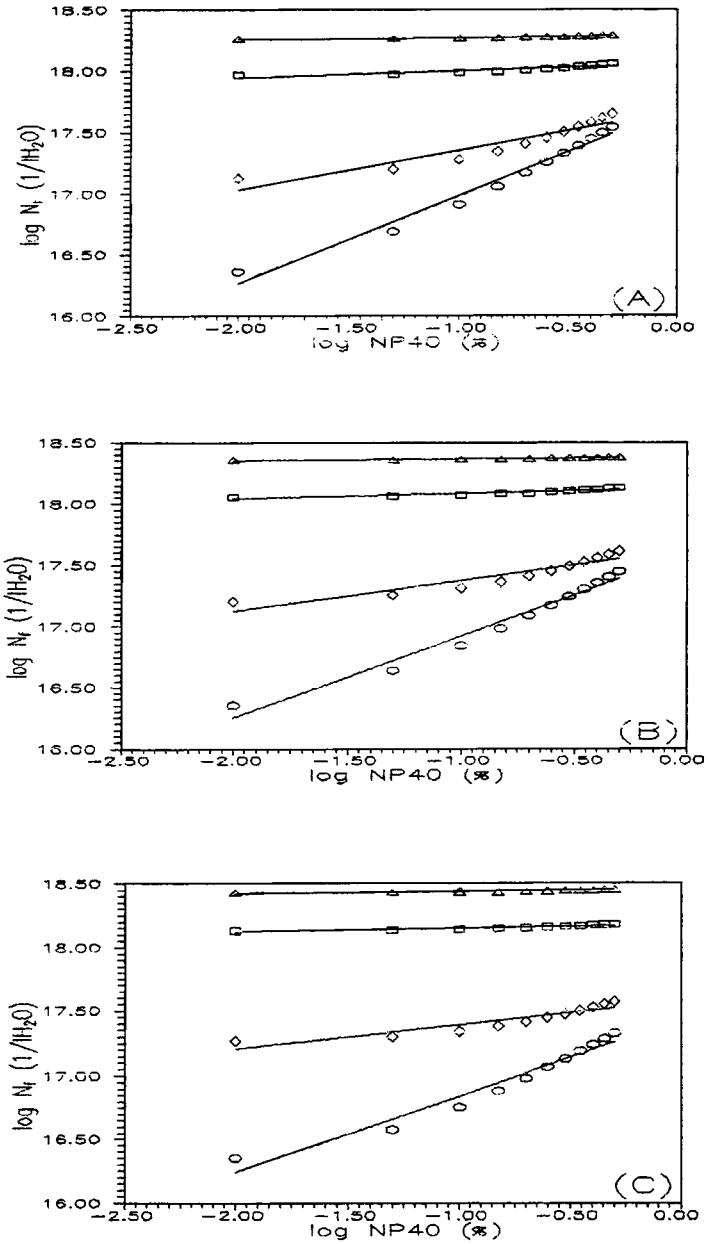

Figure 7 No. particles vs. concentration of NP-40 curves: (△) SLS = 0.5%; (□) SLS = 0.255%; (◇) SLS = 0.04%; (○) SLS = 0.01%. (A) Initiator concentration = 0.08%; (△) slope = 0.017; (□) slope = 0.056; (◇) slope = 0.321; (○) slope = 0.72. (B) Initiator concentration = 0.265%; (△) slope = 0.015; (□) slope = 0.041; (◇) slope = 0.249; (○) slope = 0.669. (C) Initiator concentration = 0.45%; (△) slope = 0.014; (□) slope = 0.03; (◇) slope = 0.184; (○) slope = 0.601.

literature.[18–20] Use of these values results in a slope of 0.410 for the log D_f-vs.-log$[1/(G_aA_a + G_nA_n)]$ plot as shown by the symbol * in Figure 9. Please note that the data points are somewhat scattered. If we set A_n equal to 0.238×10^{21} nm^2/g, the data points converge to a straight line with a slope of 0.405, as shown by the symbol ○ in Figure 9. The value of A_n obtained from our experimental data is very close to the one estimated from the literature. In addition, the slope (0.405) is slightly greater than the prediction. This is probably due to flocculation during the monomer emulsion feed.

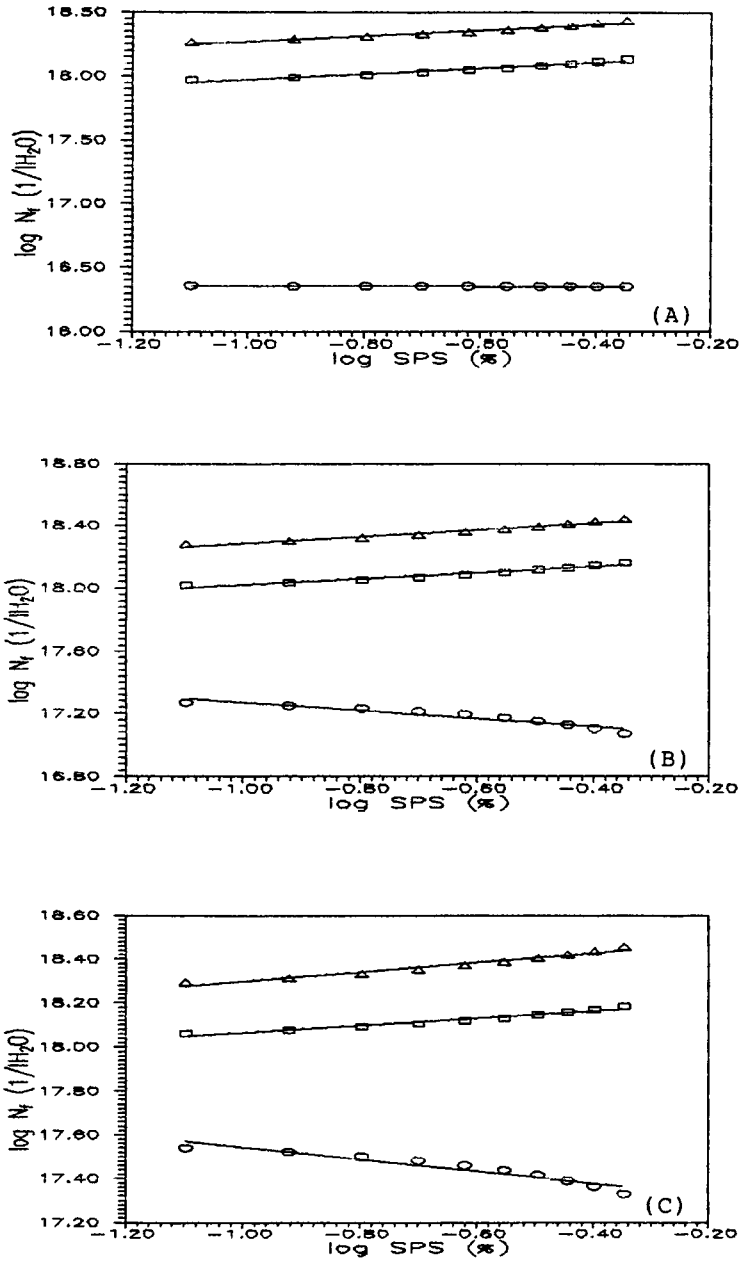

Figure 8 No. particles vs. concentration of initiator curves: (△) SLS = 0.5%; (□) SLS = 0.255%; (○) SLS = 0.01%. (A) NP-40 = 0.01%; (△) slope = 0.224; (□) slope = 0.222; (○) slope = −0.01. (B) NP-40 = 0.255%; (△) slope = 0.219; (□) slope = 0.189; (○) slope = −0.257. (C) NP-40 = 0.5%; (△) slope = 0.217; (□) slope = 0.163; (○) slope = −0.277.

Table II Calculated Parameters to Correlate Total Particle Surface Area to Surfactant Loadings

	c	α_a	b_a	α_n	b_n
MMA (Chu)	2.28×10^{21}	1.15×10^{22}	0.1584	4.94×10^{19}	2.9542
BA (Chu)	-1.75×10^{20}	9.45×10^{20}	0.3180	3.51×10^{20}	0.5560
MMA/BA (50/50)	5.29×10^{20}	1.19×10^{21}	0.5300	4.76×10^{20}	0.5000

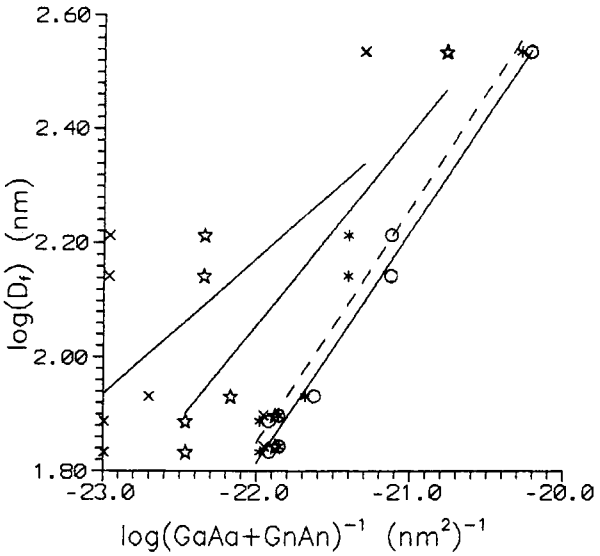

Figure 9 Final particle size vs. reciprocal of particle surface area covered by surfactants immediately after nucleation: (O) $A_n = 0.238 \times 10^{21}$, slope = 0.405; (X) $A_n = 18.3 \times 10^{21}$, slope = 0.237; (*) $A_n = 4.38 \times 10^{21}$, slope = 0.333; (*) $A_n = 0.48 \times 10^{21}$, slope = 0.41.

Fitch and Tsai[21] found oligomers with molecular weight ranging from 100 to 300 during nucleation. Figure 10 shows the GPC data of the 15 min samples. The data clearly show that low molecular weight oligomers exist and that the lower the concentration of surfactants in the initial reactor charge the more significant the low molecular weight peak. Thus, the reaction in the aqueous phase plays an important role during the early stage of polymerization. Experimental data of particle-size distribution and molecular weight distribution support the coagulative nucleation mechanism when the concentration of SLS is way below its CMC, whereas we are unable to resolve the nucleation mechanisms when the concentration of SLS is near or higher than its CMC.

The DLVO theory[22,23] predicts that increasing the ionic strength will compress the electric double layer around the particle and lead to flocculation. According to the coagulation rate expression developed by Vanderhoff et al.,[24] the flocculation tendency of the latex also increases with increasing agitation speed. The experimental data listed in Table III indicate that the particle size increases from 77.4 to 95.9 nm when the ionic strength is changed from 0.160 to 0.326%. In the experimental work, sodium chloride was added to the initial reactor charge to adjust the ionic strength. Finally, the particle size increases from 77.4 to 90.6 nm when the agitation speed is changed from 400 to 1200 rpm.

CONCLUSIONS

In the semibatch emulsion copolymerization of MMA and BA, the concentration of SLS in the initial reactor charge is the most important variable in

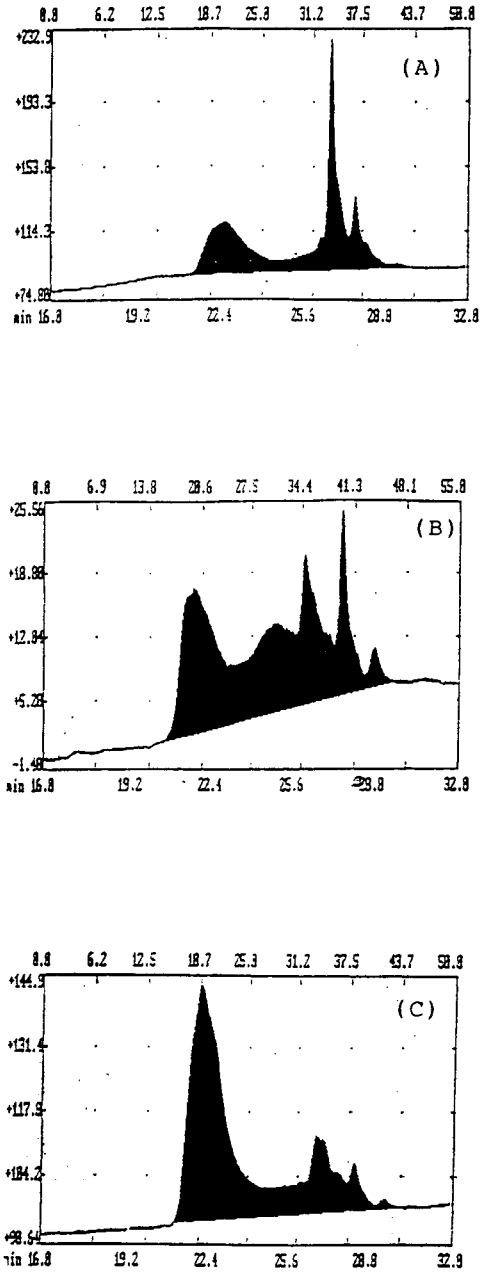

Figure 10 GPC data of 15 min samples: (A) experiment L, M_n = 98,026, M_w = 330,586, M_w/M_n = 3.37, low molecular weight oligomers 200–1000; (B) experiment M, M_n = 187,103, M_w = 430,783, M_w/M_n = 2.3, low molecular weight oligomers 200–300; (C) experiment S, M_n = 114,793, M_w = 490,947, M_w/M_n = 4.28, low molecular weight oligomers 150–1200.

Table III Effect of Ionic Strength and Agitation Speed on Latex Particle Size

Ionic Strength (%)	Agitation Speed (rpm)	Particle Size (nm)
0.160	400	77.4
0.160	800	89.4
0.160	1200	90.6
0.245	400	91.3
0.326	400	95.9

determining the particle size. NP-40 is the second most important variable and it acts as an auxiliary stabilizer. Both the initiator and monomer in the initial reactor charge and the ratio of MMA to BA show very little effect on the particle size. Experimental data also indicate that the particle size increases with increasing electrolyte concentration in the initial reactor charge and agitation speed.

Both micellar and homogeneous nucleation mechanisms predict that the number of particles nucleated is proportional to the concentration of anionic surfactant to the $\frac{3}{5}$ power. In this work, the plot of log N_f-vs.-log SLS results in a slope of 0.4–1.2, which is consistent with Feeney's results based on the coagulative nucleation mechanism. The experiment using the lowest amount of surfactants displays a positive-skew particle-size distribution immediately after nucleation is complete, which is also consistent with the coagulative nucleation. We extend the Novak model to the case of mixed surfactants and show that the slope of the log D_f-vs.-log$[1/(G_aA_a + G_nA_n)]$ plot is $\frac{1}{3}$ for the coagulative nucleation mechanism. Applying the modified Novak model to our experimental data results in a slope of 0.405. The deviation might be due to flocculation during the monomer emulsion feed. The GPC data of the 15 min samples show a low molecular weight peak. Thus, the reaction in the aqueous phase is very important during nucleation. Based on the above evidence, the semibatch emulsion copolymerization of MMA and BA follows the coagulative nucleation mechanism when the concentration of SLS is way below its CMC.

The financial support from National Science Council, Taiwan, Republic of China (NSC82-0113-E-011-170T), is greatly appreciated.

REFERENCES

1. W. D. Harkins, *J. Am. Chem. Soc.*, **69,** 1428 (1947).
2. W. V. Smith and R. W. Ewart, *J. Chem. Phys.*, **16,** 592 (1948).
3. W. V. Smith, *J. Am. Chem. Soc.*, **70,** 3695 (1948).
4. R. M. Fitch, M. B. Prenosil, and K. J. Sprick, *J. Polym. Sci. C*, **27,** 95 (1969).
5. F. K. Hansen and J. Ugelstad, *J. Polym. Sci. Polym. Chem. Ed.*, **16,** 1953 (1978).
6. C. P. Roe, *Ind. Eng. Chem.*, **60,** 20 (1968).
7. R. M. Fitch and R. C. Watson, *J. Colloid Interface Sci.*, **68,** 14 (1979).
8. G. Lichti, R. G. Gilbert, and D. H. Napper, *J. Polym. Sci. Polym. Chem. Ed.*, **21,** 269 (1983).
9. J. Ugelstad, F. K. Hansen, and S. Lange, *Makromol. Chem.*, **175,** 507 (1974).
10. J. Ugelstad, M. S. El-Aasser, and J. Vanderhoff, *J. Polym. Sci. Lett.*, **11,** 503 (1973).
11. R. W. Novak, *Adv. Org. Coat. Sci. Technol. Ser.*, **10,** 54 (1988).
12. *Strategy of Experimentation,* revised ed., E. I. du Pont de Nemours and Co., Wilmington, DE, 1987.
13. N. Sutterlin, H.-J. Kurth, and G. Markert, *Makromol. Chem.*, **177,** 1549 (1976).
14. J. W. Vanderhoff, J. F. Vitkuske, E. B. Bradford, and T. Alfrey, Jr., *J. Polym. Sci.*, **20,** 225 (1956).
15. P. J. Feeney, D. H. Napper, and R. G. Gilbert, *Macromolecules,* **17,** 2520 (1984).
16. H. H. Wang and H. H. Chu, *Polym. Bull.*, **24,** 207 (1990).
17. H. H. Chu and C. C. Lin, *Polym. Bull.*, **28,** 419 (1992).
18. N. Sutterlin, in *Polymer Colloids II,* R. M. Fitch, Ed., Plenum Press, New York, 1980, p. 583.
19. B. Kronberg and P. Stenius, *J. Colloid Interface Sci.*, **102,** 410 (1984).
20. R. J. Orr and L. Breitman, *Can. J. Chem.*, **38,** 668 (1960).
21. R. M. Fitch and C. H. Tsai, in *Polymer Colloids,* R. M. Fitch, Ed., Plenum, New York, 1971, p. 73.
22. B. V. Deryagnin and L. D. Landau, *Acta Physicochim. USSR,* **14,** 633 (1941).
23. E. J. W. Verwey and J. Th. G. Overbeek, *Theory of the Stability of Lyophobic Colloids,* Elsevier, New York, 1943.
24. J. W. Vanderhoff, in *Science and Technology of Polymer Colloids,* G. W. Poehlein, R. H. Ottewill, and J. W. Goodwin, Eds., NATO ASI Series, Martinus Nijhoff, Boston, 1983.

Received February 25, 1994
Accepted May 16, 1994